Ultrahigh-finesse, low-mode-volume Fabry–Perot microcavity

Andreas Muller,[1,*] Edward B. Flagg,[1] John R. Lawall,[2] and Glenn S. Solomon[1,2]

[1]*Joint Quantum Institute, National Institute of Standards and Technology and University of Maryland, Gaithersburg, Maryland 20899, USA*

[2]*Atomic Physics Division, National Institute of Standards and Technology, Gaithersburg, Maryland 20899, USA*

**Corresponding author: andreas.muller@nist.gov*

Received March 9, 2010; revised May 28, 2010; accepted June 12, 2010;
posted June 17, 2010 (Doc. ID 125202); published June 30, 2010

Ultralow-loss concave micromirrors with radius of curvature below 60 μm were fabricated by laser ablation and reflective coatings. A 10-μm-long microcavity with a mode volume of 40 μm^3 was set up with two such mirrors, and the cavity linewidth was measured both spectrally and temporally. The smallest linewidth obtained was 96 MHz, corresponding to a quality factor of 3.3×10^6 and a finesse in excess of 1.5×10^5. With these parameters, we estimate that a variety of solid-state quantum emitters coupled to the cavity may enter the strong coupling regime.

OCIS codes: 120.2230, 270.0270.

Traditionally used in macroscopic lasers and sensors, and more recently in microscopic semiconductor lasers [1], optical cavities are now a critical component in the rapidly growing research fields of cavity QED [2,3] and optomechanics [4]. For many applications, cavities combining large quality factor, Q, and small mode volume, V, are desirable as they offer long cavity photon lifetimes and strong circulating electric fields. For example, in cavity QED, the strong coupling between a single cavity mode and a single quantum emitter is reached when the circulating electric field is large enough such that the corresponding Rabi period is shorter than both the emitter's decoherence time and the cavity photon lifetime. In cavity optomechanics, small cavities with large Q are needed to couple to small high-frequency mechanical resonators. Integrated approaches using micropost [3,5], photonic crystal defect [6], and whispering gallery mode [7–9] resonators are thus very attractive, but they come with severe restrictions on spectral tunability. This issue is well known in VCSELs [10]. Nonetheless, low-threshold lasers [7], single-photon sources [11], and sensors [12] currently all rely on these types of microcavities.

An alternative approach is a cavity of the Fabry–Perot (FP) type based on freely movable curved mirrors [13]. It has the advantage of being fully tunable and can be mode matched to an optical fiber for efficient light collection. But while macroscopic FP cavities with a finesse exceeding 1 million have been available for over a decade [14], downscaling these cavities has been challenging because of the difficulty of fabricating microscopic concave spherical features with low enough surface roughness. Recent advances in microfabrication, along with annealing with a CO_2 laser or a gas flame, now allow micrometer feature sizes with subnanometer surface microroughness [9]. A focused CO_2 laser can also be used directly in an ablation process to simultaneously produce spherical features and anneal them. In this manner, together with the deposition of reflective coatings, mirrors of exceptionally high quality have been obtained, and cavities with a finesse as high as 37,000 and a mode volume of 600 μm^3 have been demonstrated [15]. However, although these have enabled milestone experiments in cold-atom cavity QED, the reported mirror finesse is still far from the theoretical limits imposed by surface roughness. In addition, significantly smaller mode volumes are necessary for solid-state cavity QED experiments using quantum emitters, such as single molecules [16], impurity centers [17], colloidal nanocrystals, and quantum dots [18,19].

Motivated by applications in cavity QED with semiconductor quantum dots [20,21], we have fabricated micromirrors using laser ablation with significantly improved finesse and lower mode volume. We report here the fabrication and characterization of these cavities. A surface roughness below 0.4 nm of the concave substrate combined with a high-quality dielectric coating allow us to reach a finesse exceeding 150,000; at the same time, the mode volume is only 40 μm^3 at a wavelength of $\lambda = 920$ nm. With these parameters, we calculate that, for a single quantum emitter coupled to the cavity, the strong coupling regime could be reached. Moreover, the emission may be coupled directly into a single-mode fiber.

The micromirrors were created either at the tip of single-mode fibers or on planar fused silica substrates using a CO_2 laser operating at a wavelength of $\lambda = 10.6$ μm. The laser was focused to the fiber core with a 25 mm focal length ZnSe lens and created concave features with a diameter ranging from 10 to 100 μm of the order of 1 μm deep. Typical laser powers used were of the order of 100 mW. Figure 1(a) shows an atomic force microscope (AFM) image of a laser ablated concave feature. The image reveals a smooth concave spherical surface with radius of curvature of around 30 μm and rms surface microroughness near 0.2 nm [Fig. 1(b)]. The mirrors were then coated by ion-beam sputtering with a reflective coating consisting of 44 dielectric layers of SiO_2 and Ta_2O_5, having a theoretical maximum reflectivity $R = 1 - T = 1 - 3 \times 10^{-7}$ at a wavelength $\lambda = 955$ nm. To set up a microcavity, two mirror-tipped fibers were mounted facing each other [Fig. 1(c)], onto a piezoelectric actuator. We report here measurements performed on two different microcavities (labeled "A" and "B"), consisting of two sets of similar mirrors all from the same batch.

The quality factor of a low-loss optical cavity can be accessed either in the time domain through measurements of the cavity ringdown time τ, or in the frequency

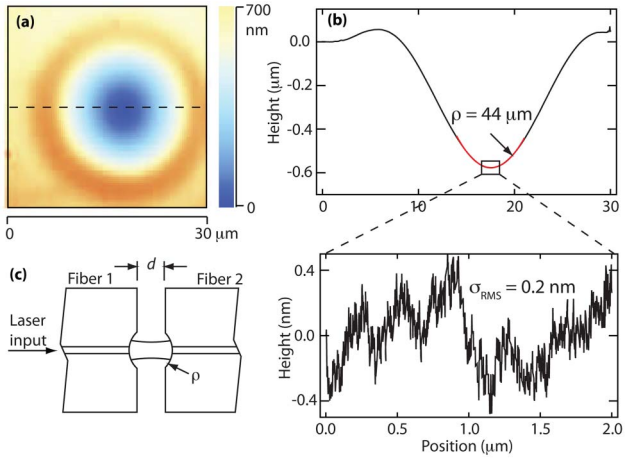

Fig. 1. (Color online) (a) AFM image of an uncoated concave precursor to a micromirror on a fused silica chip. (b) Cross-sectional height profile of the feature with a zoomed in view showing surface roughness. (c) Schematic of a microcavity consisting of two concave micromirrors (radius of curvature ρ) fabricated at the tips of single-mode fibers.

domain via the spectral linewidth. These quantities are related by $\tau = 1/(2\pi\Delta\nu)$, where $\Delta\nu$ is the FWHM of a transmission resonance. A related quantity that is independent of the cavity length is the finesse $F = \mathrm{FSR}/\Delta\nu = 2\pi/(\sum_i \Gamma_i)$, where $\sum_i \Gamma_i$ represents the sum of all round-trip fractional power losses. When the cavity consists of two identical mirrors and cavity propagation losses can be neglected, this expression reduces to $F = \pi/(T + \Gamma)$, where T denotes single-mirror transmission and Γ denotes all single-mirror losses, such as absorption and scatter, that are not due to transmission.

To determine the cavity length L and, thus, the free spectral range (FSR) $[c/(2L)]$, we make use of the resonance condition $L = N\lambda/2$ and study the change in resonant cavity length for a fixed-mode order number N for a series of different injected wavelengths. Figure 2(a) shows the transmission through cavity A for three different laser wavelengths as a function of cavity length. By tracking the mode labeled N in the figure, one infers $N \approx 23$ and a corresponding cavity length of $L \approx 10$ μm. Figure 2(b) shows both the fundamental mode of cavity B and a higher-order transverse mode as well. The frequency separation between transverse modes, δ, can be used to calculate the mirror radius of curvature $\rho = L/(2\sin^2(\pi L\delta/c))$. With ρ and $L = c/(2\mathrm{FSR})$ known, the spot size of a fundamental mode at its waist is found

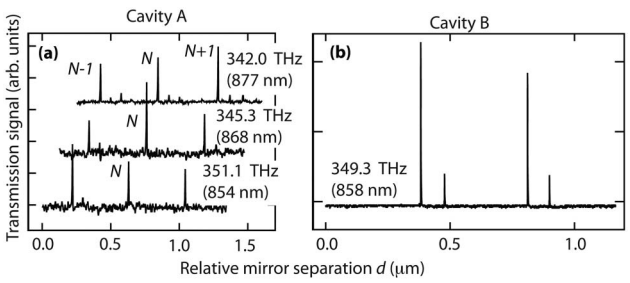

Fig. 2. (a) Transmission of cavity A as a function of relative mirror separation for three fixed laser frequencies. (b) Transmission of cavity B as a function of relative mirror separation for one fixed laser frequency.

Table 1. Summary of Cavity Parameters

	FSR	δ	L	ρ	w_0^a	V^a
Cavity A	15 000	2 300	10.3	59	2.2	40
Cavity B	12 900	3 000	11.6	44	2.1	40
Unit	GHz	GHz	μm	μm	μm	μm^3

[a]At $\lambda = 920$ nm.

as $w_0 = \sqrt{\lambda((\rho - L/2)L/2)^{1/2}/\pi}$. Finally, the mode volume is $V = \pi w_0^2 L/4$. Table 1 summarizes these values for cavities A and B. Although the fiber tips are initially in contact ($d = 0$), L inferred from FSR is of the order of 10 μm. This is primarily due to the depth of the mirrors; a depth of ≈ 3.5 μm was measured for mirrors of sizes similar to those used in cavities A and B.

The cavity linewidth, $\Delta\nu$, was measured by means of a narrowband tunable diode laser. A reflectivity measurement is shown in Fig. 3(a) at $\lambda = 940$ nm (cavity B), where $\Delta\nu = 96$ MHz and the magnitude of the dip is about 1.5%.

An independent measurement of the cavity ringdown time was made using a mode-locked picosecond-pulsed Ti:sapphire laser and a fast avalanche photodiode. A laser pulse was introduced into one of the fibers of the cavity, and the time-resolved transmission was recorded by time-correlated single-photon counting. Figure 3(b) shows the result of such a measurement, where the decay time is $\tau = 1.6$ ns at $\lambda = 925$ nm (cavity A). The corresponding linewidth $1/(2\pi\tau)$ is 100 MHz, consistent with the frequency-domain measurement.

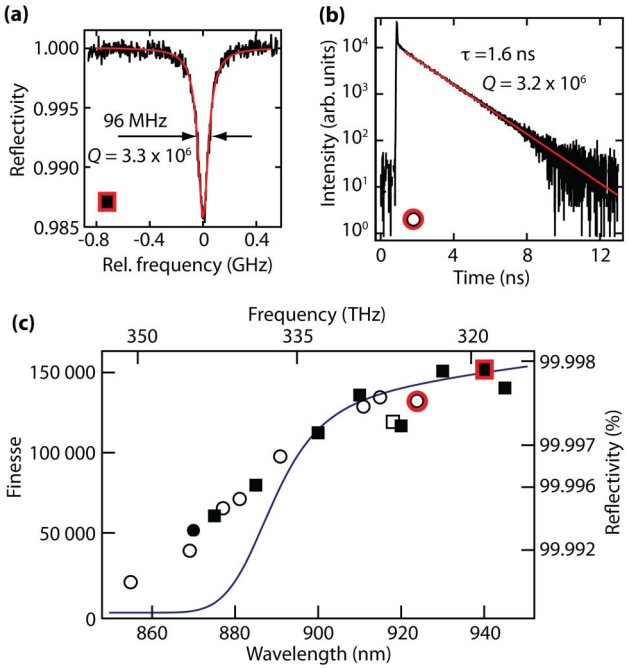

Fig. 3. (Color online) (a) Spectral reflectivity measurement of cavity B at $\lambda = 940$ nm. (b) Cavity ringdown measurement of cavity A at $\lambda = 925$ nm. (c) Summary of finesse measurements. Filled (empty) squares represent spectral (temporal) measurements of cavity A. Filled (empty) circles represent spectral (temporal) measurements of cavity B. The highlighted symbols refer to measurements in (a) and (b). The solid line is the calculated finesse.

The mirror finesse is calculated from the spectral linewidth as $F = \mathrm{FSR}/\Delta\nu$. Its values are summarized in Fig. 3(c), including spectral and temporal measurements for cavities A and B. Values for the two cavities are in close agreement. At the frequency at which the coating is maximally reflective, F is measured to be as large as 150,000, corresponding to a mirror reflectivity $R = 1 - \pi/F = 99.998\%$. This leads to a cavity quality factor $Q = \nu/\Delta\nu = 3.3 \times 10^6$ in a mode volume of only 40 $\mu\mathrm{m}^3$.

Relating the measured cavity finesse to the mirror properties via $T + \Gamma = \pi/F$, one finds that mirror transmission T is not the dominant loss mechanism limiting the finesse. Indeed, T can be calculated from the mirror layer structure to be $T \approx 3 \times 10^{-7}$ at $\lambda = 955$ nm, whereas $\pi/F \approx 2.1 \times 10^{-5}$. Taking an estimate of loss from surface roughness by the commonly used scattering factor $S(\lambda) = (4\pi\sigma_{\mathrm{RMS}}/\lambda)^2$ [22], one obtains a loss of the order of 10^{-5} with $\sigma_{\mathrm{RMS}} \approx 0.2$ nm from Fig. 1(b) at $\lambda = 920$ nm. Therefore, we conclude that roughness scattering is likely the dominant source of loss limiting the finesse. The solid curve in Fig. 3(c) is a plot of the calculated finesse $F(\lambda) = \pi/(S(\lambda) + T(\lambda))$ in which $\sigma_{\mathrm{RMS}} = 0.34$ nm is found to be the value best fitting the data. Finally, we can relate T and Γ to the depth of the reflection dip shown in Fig. 3(a). For a mode-matched input beam, $R_{\mathrm{min}} = \Gamma^2 F^2/\pi^2 \approx 1 - 2T/\Gamma = 96.6\%$ [23]. The measured value of 98.5% differs primarily due to imperfect mode matching.

Because the finesse is dominated by loss and not transmission, improved cavity finesse will require mirrors of even lower surface roughness. However, F is currently sufficiently high to explore interesting cavity QED and optomechanical phenomena. For instance, combining one of these fiber-based mirrors with a semiconductor sample consisting of quantum dots above a distributed Bragg reflector [21] would result in a fully tunable fiber integrated cavity QED system in the "good cavity limit". Previous work has focused mainly on the opposite regime [18,19], in which the cavity linewidth is much larger than the emitter linewidth. Strain-induced InAs quantum dots in an unprocessed sample may have a linewidth as low as 0.5 GHz near 4 K [21]. By extrapolating the results of [19], we can expect a Rabi splitting of 1.3 GHz in our FP microcavities with $V \approx 40$ $\mu\mathrm{m}^3$. With nanosecond-long cavity lifetimes, vacuum Rabi oscillations may be recorded directly in the time domain. Finally, the high-Q microcavity is also promising for coupling to nanoscale mechanical resonators [24], single atoms or ions [25], single molecules [16], impurity centers [17], and quantum dot nanocrystals.

We thank J. Zeng for CO_2 laser use in early stages of this work and acknowledge National Science Foundation (NSF) support through the Physics Frontier Center at the Joint Quantum Institute.

References

1. H. Soda, K. Iga, C. Kitahara, and Y. Suematsu, Jpn. J. Appl. Phys. **18**, 2329 (1979).
2. K. J. Vahala, Nature **424**, 839 (2003).
3. J. M. Gérard, B. Sermage, B. Gayral, B. Legrand, E. Costard, and V. Thierry-Mieg, Phys. Rev. Lett. **81**, 1110 (1998).
4. T. J. Kippenberg and K. J. Vahala, Opt. Express **15**, 17172 (2007).
5. G. S. Solomon, M. Pelton, and Y. Yamamoto, Phys. Rev. Lett. **86**, 3903 (2001).
6. O. Painter, J. Vučkovič, and A. Scherer, J. Opt. Soc. Am. B **16**, 275 (1999).
7. S. L. McCall, A. F. J. Levi, R. E. Slusher, S. J. Pearton, and R. A. Logan, Appl. Phys. Lett. **60**, 289 (1992).
8. V. B. Braginsky, M. L. Gorodetsky, and V. S. Ilchenko, Phys. Lett. A **137**, 393 (1989).
9. D. K. Armani, T. J. Kippenberg, S. M. Spillane, and K. J. Vahala, Nature **421**, 925 (2003).
10. M. C. Y. Huang, Y. Zhou, and C. J. Chang-Hasnain, Nat. Photon. **2**, 180 (2008).
11. P. Michler, A. Kiraz, C. Becher, W. V. Schoenfeld, P. M. Petroff, L. Zhang, E. Hu, and A. Imamoglu, Science **290**, 2282 (2000).
12. A. M. Armani and K. J. Vahala, Opt. Lett. **31**, 1896 (2006).
13. D. Kleckner, W. Marshall, M. J. A. de Dood, K. N. Dinyari, B.-J. Pors, W. T. M. Irvine, and D. Bouwmeester, Phys. Rev. Lett. **96**, 173901 (2006).
14. G. Rempe, R. J. Thompson, H. J. Kimble, and R. Lalezari, Opt. Lett. **17**, 363 (1992).
15. Y. Colombe, T. Steinmetz, G. Dubois, F. Linke, D. Hunger, and J. Reichel, Nature **450**, 272 (2007).
16. I. Gerhardt, G. Wrigge, P. Bushev, G. Zumofen, M. Agio, R. Pfab, and V. Sandoghdar, Phys. Rev. Lett. **98**, 033601 (2007).
17. Y. S. Park, A. K. Cook, and H. Wang, Nano Lett. **6**, 2075 (2006).
18. J. P. Reithmaier, G. Seogonk, A. Löffler, C. Hofmann, S. Kuhn, S. Reitzenstein, L. V. Keldysh, V. D. Kulakovskii, T. L. Reinecke, and A. Forchel, Nature **432**, 197 (2004).
19. T. Yoshie, A. Scherer, J. Hendrickson, G. Khitrova, H. M. Gibbs, G. Rupper, C. Ell, O. B. Shchekin, and D. G. Deppe, Nature **432**, 200 (2004).
20. G. Cui, J. M. Hannigan, R. Loeckenhoff, F. M. Matinaga, M. G. Raymer, S. Bhongale, M. Holland, S. Mosor, S. Chatterjee, H. M. Gibbs, and G. Khitrova, Opt. Express **14**, 2289 (2006).
21. A. Muller, E. B. Flagg, M. Metcalfe, J. Lawall, and G. S. Solomon, Appl. Phys. Lett. **95**, 173101 (2009).
22. M. Trupke, E. A. Hinds, S. Eriksson, E. A. Curtis, Z. Moktadir, E. Kukharenka, and M. Kraft, Appl. Phys. Lett. **87**, 211106 (2005).
23. J. R. Lawall, J. Opt. Soc. Am. A **22**, 2786 (2005).
24. I. Favero, S. Stapfner, D. Hunger, P. Paulitschke, J. Reichel, H. Lorenz, E. M. Weig, and K. Karrai, Opt. Express **17**, 12813 (2009).
25. M. Trupke, J. Goldwin, B. Darqui, G. Dutier, S. Eriksson, J. Ashmore, and E. A. Hinds, Phys. Rev. Lett. **99**, 063601 (2007).